---

**Article:**
Hanotu, J., Kong, D. and Zimmerman, W.B. orcid.org/0000-0001-7123-737X (2016) Intensification of yeast production with microbubbles. Food and Bioproducts Processing, 100 (Part A). pp. 424-431. ISSN 0960-3085

https://doi.org/10.1016/j.fbp.2016.07.013

---

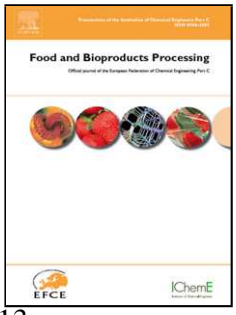


Title: Intensification of yeast production with microbubbles

Author: James Hanotu Dexu Kong William B. Zimmerman

PII: S0960-3085(16)30085-2
DOI: http://dx.doi.org/doi:10.1016/j.fbp.2016.07.013
Reference: FBP 755

To appear in: *Food and Bioproducts Processing*

Received date: 20-11-2015
Revised date: 23-7-2016
Accepted date: 26-7-2016

Please cite this article as: Hanotu, J., Kong, D., Zimmerman, W.B.,Intensification of yeast production with microbubbles, *Food and Bioproducts Processing* (2016), http://dx.doi.org/10.1016/j.fbp.2016.07.013

**Highlights**

- Yeast is known to survive and thrive within sufficient levels of dissolved oxygen
- Microbubbles transfer $O_2$ at rates superior to yeast consumption
- Cell recovery efficiency varies directly with particle size
- Particle size is a function of flocculant concentration and pH
- Enhancing yeast production is critical in consumer good production, relying on the organism

# Intensification of yeast production with microbubbles

James Hanotu[1*] Dexu Kong and William B Zimmerman[1]
[1]Department of Chemical and Process Engineering, University of Sheffield, Mappin Street, Sheffield S1 3JD, United Kingdom.
[*]Corresponding author. Email: j.hanotu@shef.ac.uk

## 1. Introduction

Yeast is the key raw material in many consumer products, for instance, in the production of beverages (Heux et al., 2006), antibiotics (Kim, 2004) and recombinant proteins (Kato et al, 1998). In addition, it plays an essential role in the energy sector for the production of biomass or biofuel. To meet the growing demand in yeast, particularly on a large scale, efficient production techniques are necessary. Yeast propagation involves growing and producing new yeast cells. It is a precursor to fermentation. While the literature on yeast fermentation is substantial, fewer studies are available on its propagation. One main reason for this lies in the challenge to keep continuous yeast cultures under aerobic conditions. Propagating yeast relies heavily on the dissolution of oxygen. Oxygen is required by yeast for the synthesis of cell membrane components (sterols) in order to regulate their mass transfer and prevent death due to malnutrition and toxicity. Sterols play a vital role in the activities of membrane bound enzymes (Hoppe & Hansford, 1984; Jahnke and Klein, 1983; Rosenfeld et al., 2003). In addition to utilising oxygen to synthesize acids such as oleic acid and linoleic acid as key cell membrane structural components (Jahnke and Klein, 1983; Rosenfeld et al., 2003), oxygen is needed for metabolic activities such as transport activity of xylose (Skoog and Hahn-Hägerdal, 1990), cell viability (Rosenfeld et al., 2003) as well as reduction of volatile *S* compounds and synthesis of mitochondrial cytochromes (Salmon et al, 1998). Another need for oxygen relates to ethanol inhibition. Hoppe and Hansford, (1984) observed that high concentration of ethanol in yeast propagation can be toxic to yeast cells. Growth rate inhibition is observed with increase in ethanol concentration (Luong 1985; Brown et al. 1981).

Despite their importance in yeast propagation, conventional aeration methods struggle to meet yeast oxygen demand particularly on a large scale. Many methods of growing yeast have been explored with the aim of efficient aeration. Mechanically stirred tank reactors (STRs) for instance, have widespread applications industrially. However, their shortcomings are due to the forced introduction of energy by stirring. As a consequence of the dissipation of energy, local environments swept by the impeller experience increased stress, which diminishes with distance away from the impeller towards the bioreactor wall. In the same vein, shear close to impeller or sparger will be high due to the direct focal transfer of momentum (Merchuk, 1991; Merchuk et al., 2002), transferring in turn, to more distant cells in the medium (Merchuk et al., 2002). The outcome of this is a wide range of variation of the shear rates with the highest shear force closest to the impeller. Consequently, heterogeneous micro environments are induced in the culture medium as well as in microbial cells. Thus imbalanced gradients in nutrient, metabolite, electrolyte and temperature levels exist in the medium influencing cell metabolism and cell morphology (Merchuk, 1991; Merchuk et al., 2002).

Airlift loop bioreactors (ALB) (Merchuk et al., 2002) were developed to overcome the challenges with stirred bioreactors. But the main engineering problem associated with conventional ALBs is their aeration mechanism. Given their importance as the main energy consuming part of the ALB, not much concern unfortunately, has been paid to this aspect of traditional ALBs. Chisti and Moo-Young (1987) grouped ALB aerators into static and dynamic spargers. Whereas static spargers use porous plates (Despande and Zimmerman, 2005a, b) or a porous baffle (Heijn en and Van't Riet, 1984) to introduce gas into liquid, dynamic spargers simply distribute gas into liquid by injecting through nozzles. In spite of the sparger type employed, conventional ALBs suffer from production of large bubbles (mm-range) and, as a consequence, due to their low residence time and low surface area to volume ratio, are inefficient in gas transfer into reactors. Zimmerman et al., (2009) proposed an improved design of the ALB, by fitting with an energy efficient microbubble generator unit. Microbubbles can rapidly improve the gaseous nutrient concentration with proper mixing, another advantage of the microbubble (Al-Mashhadani et al. 2015). Mixing is essential to keep yeast afloat, as loss by death occurs when cells sink and remain at the bottom of the reactor. Usually, sinking results from low flows and is prominent in dead zones - areas in a culture medium with minimal or no circulation. Increase in organic matter in these areas will obviously have ill effects on the entire culture due to anaerobic decomposition, bringing about reduction in yeast viability. Another reason why efficient mixing is sought is to maintain a balanced distribution of gases. As yeast metabolises, gaseous and nutritional gradients are often formed around individual cells. These gradients impose limitations on growth rate. With microbubbles, efficient mixing is achieved to overcome this setback. Zimmerman et al., (2011a) have reported higher yield with the ALB equipped with the fluidic oscillator for bubble generation in algal culture compared to conventional ALBs that produce coarse bubbles. Using the same facility, Al-Mashhadani et al. (2011) also recorded increased performance for $CO_2$ mass transfer.

The fundamental problems relating to yeast harvesting after propagation are equally challenging but not insurmountable as tuning the bubble size to match the size range for particle harvesting can mitigate both the capital and operating costs (Zimmerman et al., 2011), whilst ensuring high recovery efficiency (Hanotu et al., 2012). With microbubble production by fluidic oscillation, this is achievable by either using an appropriate sparger or better yet, adjusting the oscillation frequency. In this experimental work, we explore two critical aspects of yeast production - propagation and harvest. In doing so, we contrast in the first sections, the effect of aeration on yeast growth in an ALB, using two sparging techniques – conventionally generated bubbles and fluidic oscillator generated microbubbles - and also test the effect of varying gas supply rates under both aeration methods. Finally in the last sections, cell recovery by microflotation is investigated and presented.

## 2. Materials and Methods

### 2.1 Yeast Strain and Growth conditions

Yeast strain (*Saccharomyces cerevisiae*) was propagated in a 3 L cylindrical Airlift Loop Bioreactor (ALB) made of perspex measuring 0.3 m and 0.14 m in height and base respectively (Fig. 1). The reactor was fitted with a microporous sparger for bubble generation. The ALB supported pH, temperature and DO probes (Mettler Toledo, UK). The culture temperature was regulated using a water bath operating at (35 $^{o}$C). Sterile YPD broth (Sigma Aldrich, UK) with an extract composition of 40 % α-D-Glucose, 40 % Peptone and 20 % Yeast extract was used for the experiment. Prior to culturing, medium was autoclaved for 15 min at 121 °C. Next, three (3) litres of growth medium was pre-aerated with air bubbles for 30 min. Activation of the dried yeast was important prior to pitching. For the 3 L reactor, 2.5 g (dry cell mass) of yeast was rehydrated with 25 ml of distilled water at 32 $^{o}$C, resulting in an initial concentration of ~0.83 mg/mL. After 15 min without stirring, the yeast was then gently stirred before topping up by adding small increments of medium for 5 min.

#### 2.1.1 Biomass Concentration

Biomass concentration correlates with optical density (OD) and was measured by spectrophotometer DR 2800 (Hach Lange, UK) to determine optical density at 660 nm with sampling done hourly. Average growth rate (mg/h) after 6 h was determined using the equation 1 below:

$$C_{AV} = (C_F - C_I)/t \qquad (1)$$

where $C_F$ and $C_L$ are the initial and final biomass concentrations (mg/mL) respectively and $t$, culture time (hours).

#### 2.1.2 Aeration

Microfiltered air was sparged through a microporous sparger under oscillatory condition with average bubble diameter ~300 microns (Zimmerman et al., 2011a) and steady flow condition with average bubble diameter ~ 3 mm. Experiments were conducted under varying flowrates (0.1, 0.3, 0.5, 0.7 and 0.9) L/min for both oscillatory and continuous flow conditions for ~6 hrs.

#### 2.1.3 Determination of $K_{La}$

Based on the metabolic oxygen uptake rate of the organism during propagation, the overall oxygen transfer coefficient was determined by the yield coefficient method. Here, the dissolved $O_2$ level was recorded (in the liquid medium without yeast) until 200 s after which no increase in $O_2$ was observed, suggesting saturation. The oxygen transfer rate was then calculated using equation 2 below:

$$\frac{dC_L}{dt} = k_L a\,(C^* - C_L) \qquad (2)$$

where $K_{La}$ is the mass transfer coefficient, $C^*$, oxygen concentration at saturation conditions (mol/l); and $C_L$, oxygen concentration in the culture medium (mol/l).

### 2.2 Yeast recovery

The method applied here is similar to the microflotation method previously reported in Hanotu et *al*, (2012, 2013 and 2014). After culture, the medium pH was adjusted to 5 and 7 respectively followed by the addition of chitosan for cell agglomeration at varying concentrations: (0, 0.2, 0.4, 0.6, 0.8, 1, 1.2 %v/v). Coagulation and flocculation followed at 250 rpm and 100 rpm, for 15 and 5 min respectively, before pumping the broth at 0.5 L/min into the flotation column. Next, fluidic oscillator generated microbubbles are introduced from the bottom of the flotation column.

## 3. Results and Discussion

### 3.1 Dissolved Oxygen (DO) Level

Figure 2 presents the result of dissolved oxygen levels during propagation. The profile with microbubbles (Fig 2d) shows however, a rich supply of oxygen during growth. Except for 0.1 and 0.3 L/min when the DO dropped and remained at 1 mg/L after the 5$^{th}$ hour, DO levels remained significantly higher under all flow rates above 0.5 L/min. Interestingly, the DO level was observed to remain steady within 8-10 mg/L after 5 hours for flow rates 0.7 and 0.9 L/min. By contrast, results with coarse bubbles revealed poor supply of oxygen across all flowrates. The oxygen level in the reactor was completely consumed after just 1 hour of culture, leaving the culture oxygen deficient for the duration of the culture period. It is worthy of mention that the culture medium was pre-aerated for 30 min prior to pitching the yeast cells. During this period, the pressure in the airtight bioreactor increased (value not recorded), exceeding atmospheric pressure and consequently resulting in the initial high level of dissolved oxygen recorded.

Essentially, the level of oxygen dissolved in yeast propagation cultures mainly depends on three fundamental processes: the rate of oxygen transfer to the liquid continuous phase, the rate of oxygen transfer from the medium to the yeast cell and the rate of oxygen consumption by the yeast cells. Apparently, the most crucial process is the dissolution of oxygen. Due to the low dissolved oxygen level recorded under conventional aeration, the mass transfer coefficient results presented in Fig. 3 are calculated for only conditions under fluidic oscillator generated bubbles. The increased oxygen dissolution and level in the culture is due to the high surface area and residence time provided by the microbubbles. Whereas aerobic conditions were maintained throughout the propagation period under microbubble sparging, the reverse effect occurred under coarse bubble aeration. Microbubble sparging provide laminar flow, ensuring harmless suspension of cells in the medium and consequently, reducing dead zones. Further, the immediate vicinity around the individual yeast cell, where toxic levels are high due to the accumulation of by products, is effectively offset by microbubble sparging. There is also, effective aeration regulation of yeast heat levels.

Additionally, the rate of increase in dissolved $O_2$ was influenced by the aeration flowrate but equally, by the mixing effect brought about by the gas lift-loop mechanism of the ALB. Because ALBs undergo pneumatic agitation, they are referred to and imagined as a type of bubble column (Zimmerman et al., 2009). The pressure-driven circulatory motion owing to the design is the key reason for their inclusion in many new reactor designs in contrast to stirred tank reactors,

where the introduction of energy via impellers limit reactor yield.

### 3.2 Biomass Concentration

Figure 4 presents results of yeast growth expressed as biomass concentration. The graphs show similarity in growth pattern for both aeration techniques. Under both sets of experiment, the biomass concentration increased with increasing oxygen supply during the log phase. Highest biomass concentration (2.53 mg/mL and 2.88 mg/mL) after 6-hour propagation period (log phase) was recorded for coarse bubble and microbubble aeration systems respectively at the highest aeration rate studied. Under the lowest microbubble aeration flowrate (0.1 L/min) however, the biomass concentration achieved (2.56 mg/mL ($\pm$ 0.02)) was higher compared with that (2.53 mg/mL) obtained under highest coarse bubble aeration flowrate studied (0.9 L/min). Sparging with microbubbles at low flowrates transferred oxygen efficiently than with coarse bubbles. Further, the average growth rate with microbubbles was 0.26 mg/h, while 0.22 mg/h was recorded for coarse bubbles. The difference in maximum average growth rate result shows that microbubble aeration (0.31 mg/h $\pm$ 0.02) was 18 % more efficient than coarse bubble aeration (0.22 mg/h $\pm$ 0.01).

The mass transfer rate with coarse bubbles was significantly below the yeast oxygen uptake rate. Compared to microbubbles, the diffusive mass transfer from coarse bubbles is low (Zimmerman et al., 2009; Al-Mashhadani et al., 2011), resulting in a metabolic switch - from an oxidative state (only several minutes following pitching) to an oxido-reductive metabolism (during lag phase) (Sonnleitner and Hahnemann 1994; Rosenfeld and Beauvoit 2003). At this stage, cell viability and growth rate is low, hence the relatively low biomass yield (Brown et al. 1981). Furthermore, the limitation of growth rates at high yeast concentrations is also due to the strong inhibitory effect of ethanol (Luong 1985; Brown et al. 1981) and dissolved $CO_2$, which are the product of yeast at insufficient oxygen supply, as diffusive mass transfer is very slow, and removal of the dissolved $CO_2$ is limited by diffusion boundary layers near the bubble and at the air-liquid interface. Sonnleitner and Hahnemann (1994) confirmed that one disadvantage of the presence of ethanol in yeast propagation is its suppressive effect on yeast respiration.

Sparging with microbubbles substantially enhanced $O_2$ dissolution due to the high surface area to volume ratio effect at rates equal or higher than yeast uptake rate. Microbubbles create a rapid influx of $O_2$, but simultaneously, due to the high mass transfer coefficient and $CO_2$ gradient between the phases extract ethanol and dissolved $CO_2$, so that the bubbles bursting at the top surface completely bypass the boundary layer limitations. The improved growth rate is attributable to increased dissolved gas levels due to superior mass transfer coefficients of microbubbles. This finding corroborates results from Rosenfeld et al., (2003) where the authors observed increased cell viability at higher oxygen level.

Although the ethanol level was not measured in this study, yeast generally tends to switch from aerobic to anaerobic metabolism under insufficient oxygen supply. Given this condition, slow growth is observed as yeast cells are unable to utilize nutrients to develop sufficient cell mass but rather switch metabolic pathway to the production of ethanol and $CO_2$. The deficiency in oxygen supply causes yeast cell damage and affects yeast metabolism.

## 4. Yeast Biomass Recovery

Propagated cells are recovered/harvested for fermentation or for further downstream application/processing. Typically, centrifugation is the method employed for yeast recovery. There are two disadvantages with the method however, viz - shearing of cells (Chlup et al 2008) and the high operating cost of centrifugation (Xu et al 2005). The latter is critical on an industrial scale but the cell loss owing to cell surface disruption can pose significant losses on a molecular level. In flotation, microbubbles are exploited as a non-intrusive driver for separation. The study results showing recovery efficiency are presented in the subsequent sub-sessions.

### 4.1 Electrophoretic Mobility Analysis

Cell surface charge can be influenced by culture age and environment, which in turn can influence their harvest from the culture medium. To ascertain these effects on cell surface charge, electrophoretic mobility (EPM) was conducted by assaying propagated cells at different pHs and times (stages) during propagation. At $t_0$, the EPM of the cells was analysed between pH 2 and pH 10 in 100 mM potassium chloride. A representative set of EPM values as a function of pH is given in Figure 5. The culture samples were also collected during propagation at the logarithmic phase (7 hours post inoculation) and stationary phase (17 hours post inoculation).

In all the conditions analysed, the isoelectric point (IEP) of the cell was not reached, indicating that the cell surface is likely composed primarily of anionic moieties such as phosphates and carboxylates found in polysaccharides. Since information on the isoelectric point was not obtained, subsequent conditions and replicates were assayed only at the relevant pH i.e. 5, 7 and 9. The results obtained revealed only a slight change across the different pH environments measured. Also, the age (7 and 17 hour post inoculation) showed no significant difference in the cells zeta potential. The calculation of zeta potentials using the Smoluchowski approximation, shows that the zeta potential of the cell surface ranged between -8 and -18 mV across the various culture conditions, suggesting that the yeast suspensions in 100 mM KCl were unstable and likely to sediment over time.

### 4.2. Cell Size Characterization

When majority of the cells are still suspended, flocculation is facilitated with the addition of a coagulant/flocculant. Any flocculating agent can be used for agglomeration purposes depending on the desired end result. The result presented (see Figure 6) reveals a significant difference in cell (particle) size under the different pH conditions examined. Larger flocs were formed under pH 7 than at pH 5. In addition, there seems to be a threshold beyond which floc size decreases after approaching optimal condition. This concentration was observed in this study at 0.6 %v/v for pH 5 by contrast, at 1 %v/v for pH 7.

Over-dosing leads to particle (cell) surface charge reversal and as a consequence, re-stabilisation of the yeast cells in the culture medium. Conversely, under-dosing can result in poor particle destabilization or charge neutralisation. The narrow window of flocculation possibility exhibited under pH 5 is improved under pH 7, where higher tolerance to the biological flocculant is obtained as well as improvement on particle size.

### 4.3. Recovery efficiency

Microbubbles can serve as an effective tool in separating particles from a liquid medium. Using sub-100 μm sized bubbles generated by fluidic oscillation, yeast cells were recovered from their culture medium. Under optimum flocculant dosage, the result presented in Figure 7 shows a slight drop in recovery efficiency from 98.1 %, at pH 5 than at pH 7, which produced a recovery efficiency of 99.2 %. It is worthy of mention that the recovery efficiency was slightly different under the pH conditions investigated with neutral pH, favouring cell recovery than acidic pH.

The difference in recovery efficiency at both pHs, can be attributed to the difference in particle size under pH 5 and 7. Generally, recovery efficiency increases with particle size, until a limit is reached where the particle size drops, resulting in a corresponding drop in recovery. This pattern also correctly mirrors the relationship between particle size and coagulant concentration (see figure 6). It would seem that the closer to the IEP the particle surface charge is, the higher the recovery efficiency would be. The result here however, offers a broader insight. Charge neutralisation and/or suppression is hardly the sole factor influencing particle recovery rate and efficiency (% yield) from liquid medium; neither is the pH nor coagulant type. Microbubble role can be equally if not more crucial, with bubble size and flux (~50 μm ±10 and $15x10^4/m^3$ respectively in this study), its two rate limiting properties.

The cost of chitosan varies depending on purity. Chitosan is more expensive than conventional inorganic coagulants such as aluminium sulphate but its value is its food-friendly nature. The price for chitosan used in this study is £47.50 for 50 g (Sigma Aldrich, UK). To achieve ~ 99 % yeast recovery/harvest, 0.2 g was used per batch. This converts to 18.8 p chitosan per harvest batch. Conversely, the energy requirements are calculated assuming the following: a recovery time of 20 min, 99 % recovery efficiency and an electricity cost of 12.8 p/KWh. Therefore, the cost of harvesting per batch is estimated as 1.88 p, which translates to 0.7 KWh/kg of yeast. This estimate is based on the lab bench scale microflotation and an operating pressure of ~1 bar. The direct bubble-based separation system comparable to the microflotation system is dissolved air flotation (DAF), which operates at substantially higher pressure levels (~6 bars) (Edzwald, 2010) and consequently, higher energetics.

## 5. Future Perspective

The key challenges facing yeast production has been addressed using a low-cost ALB and an adjoining flotation cell both powered by a microbubble generation unit. Microbubble application in yeast propagation significantly increases oxygen dissolution rates, facilitating other oxygen-dependent metabolic activities. The high surface to volume ratio is the key to their increased mass transfer rate, in addition to offering high residence time coupled with low convective force that is gentle on microbial cell wall. However, further work is required to provide physiological calibration of the microbubble technology to determine its benefits in bioreactor design for both aerobic microbial propagation and anaerobic fermentation. Conversely, in flotation, there are essentially two reasons for the application of a flocculating agent: 1) suppressing cell size enough for particle-particle agglomeration 2) decreasing cell surface charge magnitude for bubble-particle contact. One recent concept is to miniaturise the bubbles to match particle size

but the physicochemical and electrochemical aspects are similarly vital. If bubble surface properties are engineered so that the surface charge magnitude is tuneable to induce bubble-particle attraction, perhaps particles recovery will occur. Additionally, introducing a gaseous flocculant via microbubbles is another approach as both agglomeration and recovery can be achieved in one processing unit. This has the benefit of completely bypassing conventional flocculating agents, decreasing contamination and ultimately saving cost.

## 6. Conclusions

The performance of two aeration techniques for yeast propagation has been studied as well as its recovery after growth. The dissolved oxygen levels, $k_{La}$ and biomass yield provide significant information on the efficiency of the aeration methods – coarse bubbles and microbubbles. The limitation of cell growth under conventional sparging method is as a consequence of oxygen deficiency in the bioreactor. In the absence of sufficient oxygen, yeast cells revert metabolism from aerobic to anaerobic, changing growth pattern as well as end products. The growth rate was improved in the presence of rich oxygen supply with microbubbles but more interestingly, the culture was maintained under aerobic conditions throughout the propagation period. Additionally, microbubble application for yeast recovery showed high recovery efficiency, with recovery efficiency varying directly with particle size.

**Acknowledgements**

WZ would like to acknowledge support from the Concept Fund of Yorkshire Forward and the EPSRC (grant no. EP/I019790/1 and EP/N011511/1). WZ would like to acknowledge the Royal Society for a Brian Mercer Innovation award. JOH would like to thank the University of Sheffield for a doctoral scholarship and the EPSRC for equipment support through the equipment loan pool scheme. Helpful discussions and support from Peter Sandfort of KATZEN Int'l are acknowledged. Many thanks also to Vaclav Tesar and Hemaka Bandulasena for helpful discussions.

## References

AL-MASHHADANI, M. K. H., BANDULASENA, H. C. H. & ZIMMERMAN, W. B. 2011. CO2 Mass Transfer Induced through an Airlift Loop by a Microbubble Cloud Generated by Fluidic Oscillation. *Industrial & Engineering Chemistry Research,* 51**,** 1864-1877.

AL-MASHHADANI, M. K. H., WILKINSON, S. J. & ZIMMERMAN, W. B. 2015. Airlift bioreactor for biological applications with microbubble mediated transport processes. *Chemical Engineering Science,* 137**,** 243-253.

BROWN, S. W., OLIVER, S. G., HARRISON, D. E. F. & RIGHELATO, R. C. 1981. Ethanol inhibition of yeast growth and fermentation: Differences in the magnitude and complexity of the effect. *European journal of applied microbiology and biotechnology,* 11**,** 151-155.

BROWN, S. W., OLIVER, S. G., HARRISON, D. E. F. & RIGHELATO, R. C. 1981. Ethanol inhibition of yeast growth and fermentation: Differences in the magnitude and complexity of the effect. *European journal of applied microbiology and biotechnology,* 11**,** 151-155.

CHISTI, M. & MOO-YOUNG, M. 1987. Airlift reactors: characteristics, applications and design considerations. *Chemical Engineering Communications,* 60**,** 195-242.

CHLUP, P. H., BERNARD, D. & STEWART, G. G. 2008. Disc Stack Centrifuge Operating Parameters and Their Impact on Yeast Physiology. *Journal of the Institute of Brewing,* 114**,** 45-61.

DESHPANDE, K. B. & ZIMMERMAN, W. B. 2005. Experimental study of mass transfer limited reaction,Part I: Use of fibre optic spectrometry to infer asymmetric mass transfer coefficients. *Chemical Engineering Science,* 60**,** 2879-2893.

DESHPANDE, K. B. & ZIMMERMAN, W. B. 2005. Experimental study of mass transfer limited reaction,Part II: Existence of cross-over phenomenon. *Chemical Engineering Science,* 60**,** 4147-4156.

EDZWALD, J. K. 2010. Dissolved air flotation and me. *Water Research,* 44**,** 2077-2106.

HANOTU, J., KARUNAKARAN, E., BANDULASENA, H., BIGGS, C. & ZIMMERMAN, W. B. 2014. Harvesting and dewatering yeast by microflotation. *Biochemical Engineering Journal,* 82**,** 174-182.

HANOTU, J., BANDULASENA, H. C. H., CHIU, T. Y. & ZIMMERMAN, W. B. 2013. Oil emulsion separation with fluidic oscillator generated microbubbles. *International Journal of Multiphase Flow,* 56**,** 119-125.

HANOTU, J., BANDULASENA, H. C. H. & ZIMMERMAN, W. B. 2012. Microflotation performance for algal separation. *Biotechnology and Bioengineering,* 109**,** 1663-1673.

HEIJNEN, J. J. & VAN'T RIET, K. 1984. Mass transfer, mixing and heat transfer phenomena in low viscosity bubble column reactors. *The Chemical Engineering Journal,* 28**,** B21-B42.

HEUX, S., CACHON, R. & DEQUIN, S. 2006. Cofactor engineering in Saccharomyces cerevisiae: Expression of a H2O-forming NADH oxidase and impact on redox metabolism. *Metabolic Engineering,* 8**,** 303-314.

HOPPE, G. & HANSFORD, G. 1984. The effect of micro-aerobic conditions on continuous ethanol production by Saccharomyces cerevisiae. *Biotechnology Letters,* 6**,** 681-686.

JAHNKE, L. & KLEIN, H. P. 1983. Oxygen requirements for formation and activity of the squalene epoxidase in Saccharomyces cerevisiae. *Journal of Bacteriology,* 155**,** 488-492.

JOSÉ, M., C., J., YUNGER & R. 1990. *The role of the gas-liquid separator of airlift reactors in the mixing process,* Kidlington, ROYAUME-UNI, Elsevier.

KATO, A., NAKAMURA, S., IBRAHIM, H., MATSUMI, T., TSUMIYAMA, C. & KATO, M. 1998. Production of genetically modified lysozymes having extreme heat stability and antimicrobial activity against Gram negative bacteria in yeast and in plant. *Food /*

*Nahrung,* 42**,** 128-130.

KIM, J.-S., AKEPRATHUMCHAI, S. & WICKRAMASINGHE, S. R. 2001. Flocculation to enhance microfiltration. *Journal of Membrane Science,* 182**,** 161-172.

KIM, M. D., LEE, T. H., LIM, H. K. & SEO, J. H. 2004. Production of antithrombotic hirudin in GAL1-disrupted Saccharomyces cerevisiae. *Applied Microbiology and Biotechnology,* 65**,** 259-262.

LUONG, J. 1985. Kinetics of ethanol inhibition in alcohol fermentation. *Biotechnology and bioengineering,* 27**,** 280-285.

MERCHUK, J. C. & GLUZ, M. 2002. Bioreactors, Air-lift Reactors. *Encyclopedia of Bioprocess Technology.* John Wiley & Sons, Inc.

ROSENFELD, E. & BEAUVOIT, B. 2003. Role of the non-respiratory pathways in the utilization of molecular oxygen by Saccharomyces cerevisiae. *Yeast,* 20**,** 1115-1144.

ROSENFELD, E., BEAUVOIT, B., BLONDIN, B. & SALMON, J.-M. 2003. Oxygen consumption by anaerobic Saccharomyces cerevisiae under enological conditions: effect on fermentation kinetics. *Applied and environmental microbiology,* 69**,** 113-121.

SALMON, J.-M., FORNAIRON, C. & BARRE, P. 1998. Determination of oxygen utilization pathways in an industrial strain of Saccharomyces cerevisiae during enological fermentation. *Journal of Fermentation and Bioengineering,* 86**,** 154-163.

SKOOG, K. & HAHN-HÄGERDAL, B. 1990. Effect of oxygenation on xylose fermentation by Pichia stipitis. *Applied and environmental microbiology,* 56**,** 3389-3394.

SONNLEITNER, B. & HAHNEMANN, U. 1994. Dynamics of the respiratory bottleneck of Saccharomyces cerevisiae. *Journal of Biotechnology,* 38**,** 63-79.

XU, T. J., ZHAO, X. Q. & BAI, F. W. 2005. Continuous ethanol production using self-flocculating yeast in a cascade of fermentors. *Enzyme and Microbial Technology,* 37**,** 634-640.

ZIMMERMAN, W. B., HEWAKANDAMBY, B. N., TESAŘ, V., BANDULASENA, H. C. H. & OMOTOWA, O. A. 2009. On the design and simulation of an airlift loop bioreactor with microbubble generation by fluidic oscillation. *Food and Bioproducts Processing,* 87**,** 215-227.

ZIMMERMAN, W. B., ZANDI, M., HEMAKA BANDULASENA, H. C., TESAŘ, V., JAMES GILMOUR, D. & YING, K. 2011. Design of an airlift loop bioreactor and pilot scales studies with fluidic oscillator induced microbubbles for growth of a microalgae Dunaliella salina. *Applied Energy,* 88**,** 3357-3369.

## Figures

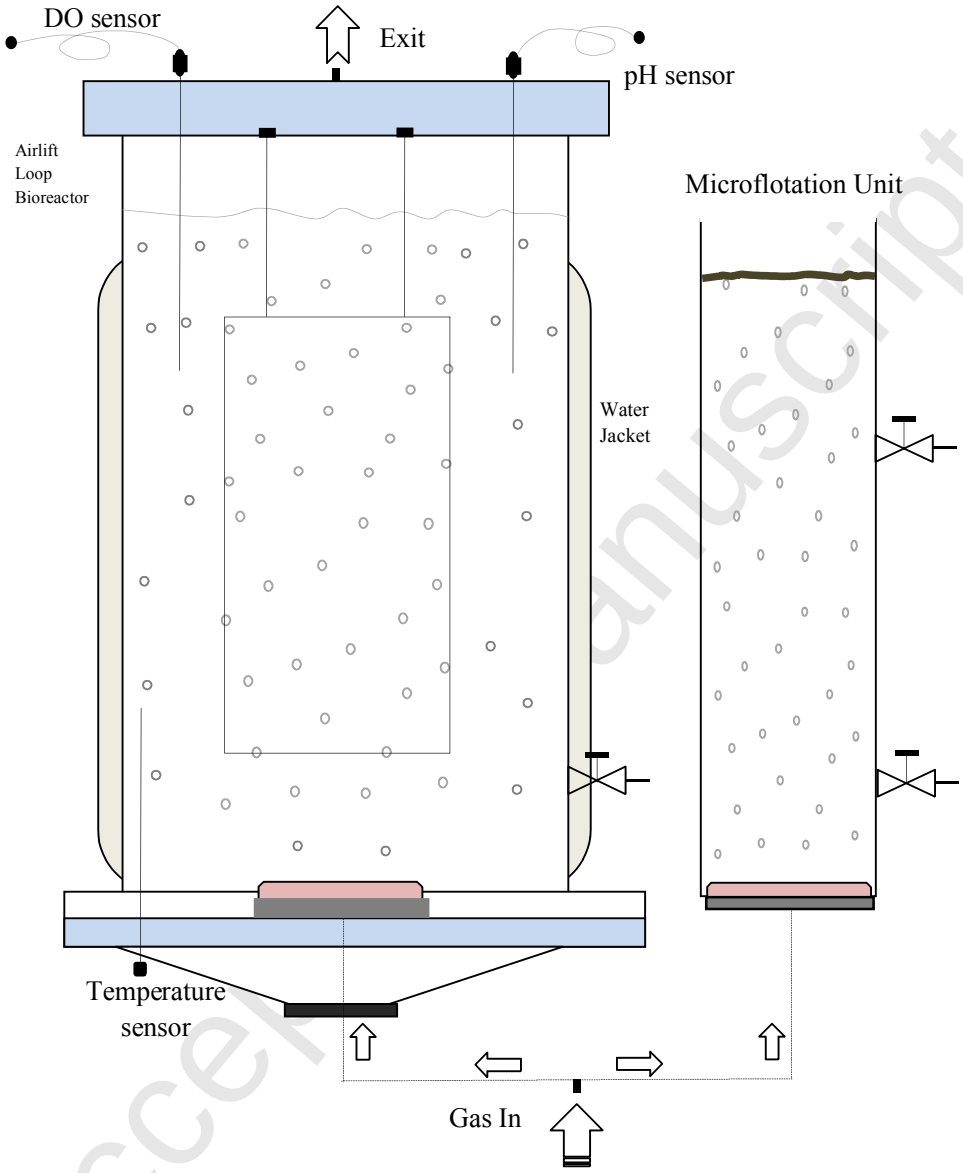


**Figure 1:** Schematic representation of the Airlift Loop Bioreactor. Microfiltered air was supplied through the sparger for bubble generation. The ALB is also fitted with a pH and a DO probe, placed from the top to mid-way in the bioreactor while a thermocouple is inserted from the reactor bottom. A water-jacket is incorporated to regulate the culture temperature.

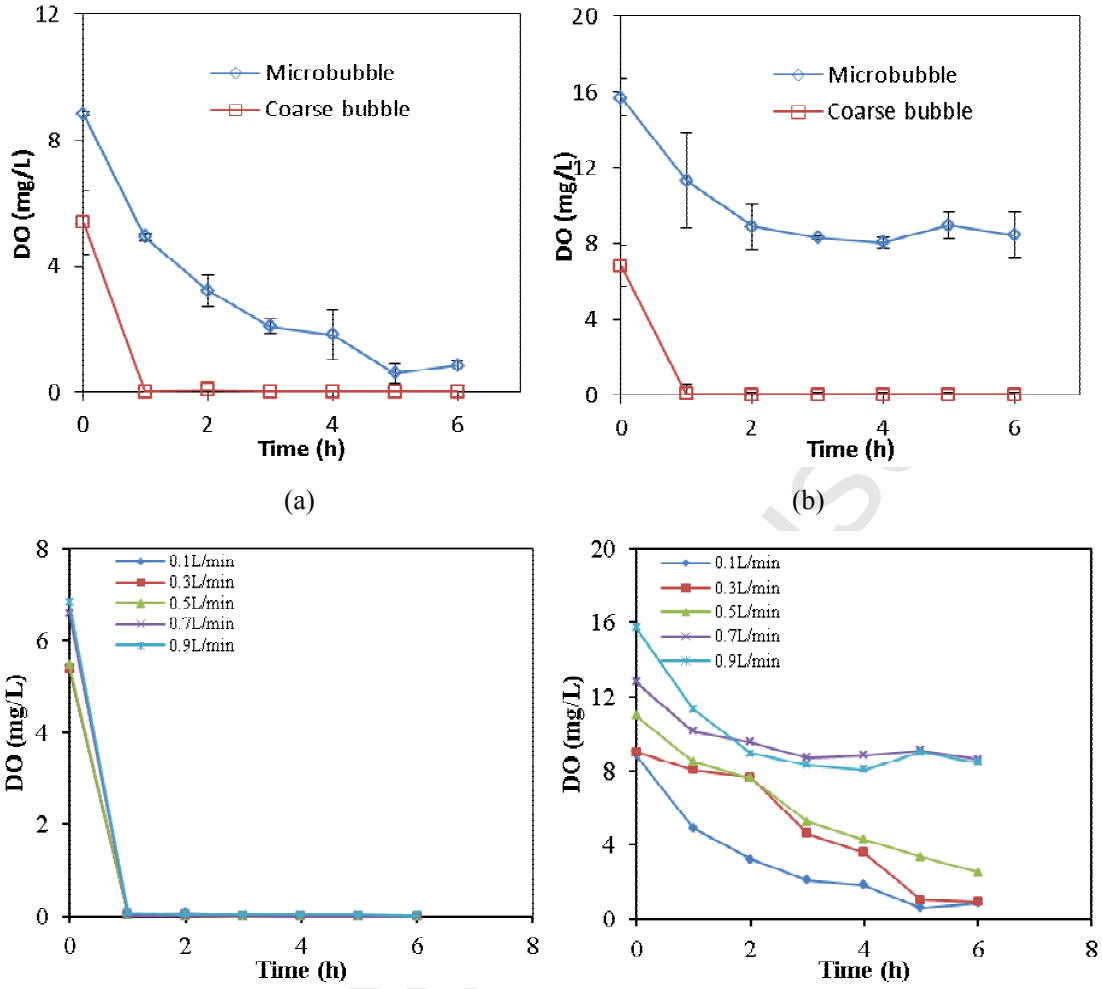


**Figure 2**: Graph of dissolved oxygen level against time during yeast propagation. Dissolved oxygen level plot of microbubbles and coarse bubble aeration systems (a) Lowest flowrate studied – 0.1 L/min. (b) Highest flowrate studied– 0.9 L/min. Combined plot of oxygen concentration at varying flowrates: (c) With coarse bubbles. (d) With microbubbles. Under coarse bubble aeration, the culture was oxygen deficient after 1 hour of propagation while the reverse was largely the case under microbubble aeration. The error bar represents standard error for the duplicated tests.

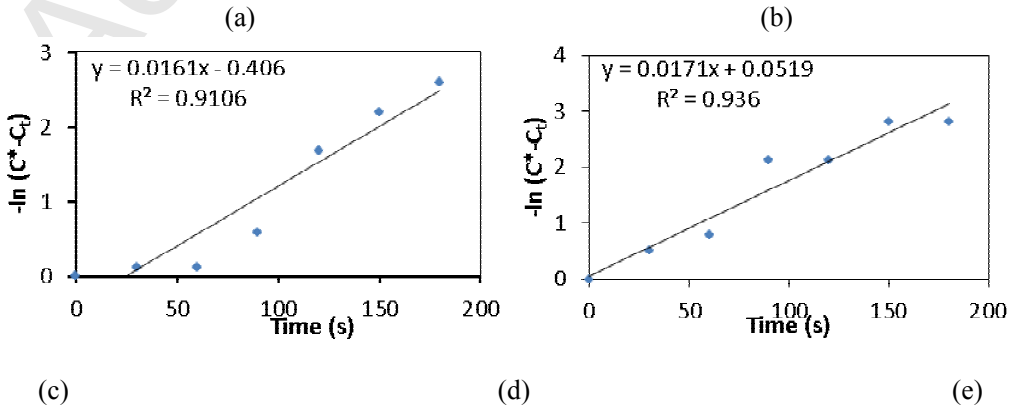

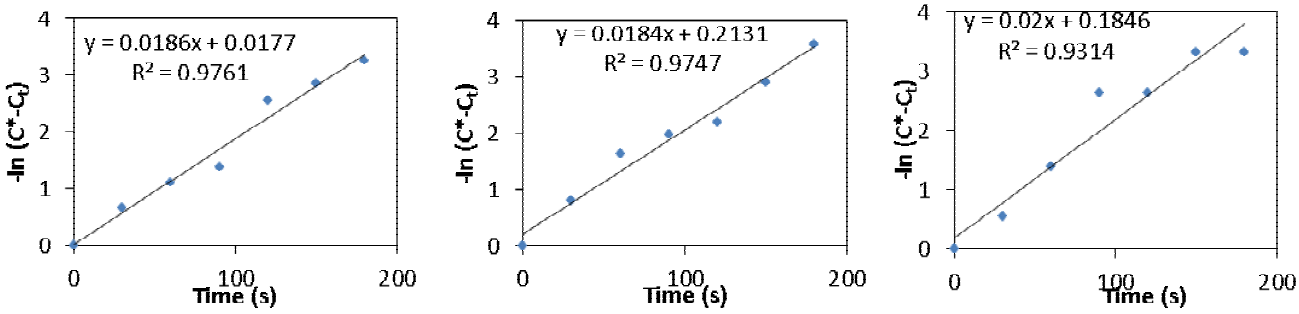


**Figure 3**: Plots of microbubble mass transfer rate against time at varying flowrate. Rate of oxygen transfer increased directly with increase in flow rate (Q). (a) Q = 0.1 L/min; $k_La$ = 0.0161 Hz (b) Q = 0.3 L/min; $k_La$ = 0.0171 Hz (c) Q = 0.5 L/min; $k_La$ = 0.0186 Hz (d) Q = 0.7 L/min; $k_La$ = 0.0184 Hz (e) Q = 0.9 L/min; $k_La$ = 0.02 Hz. Dissolved $O_2$ level in the liquid medium increased continuously with time and reached saturation at 200 s.

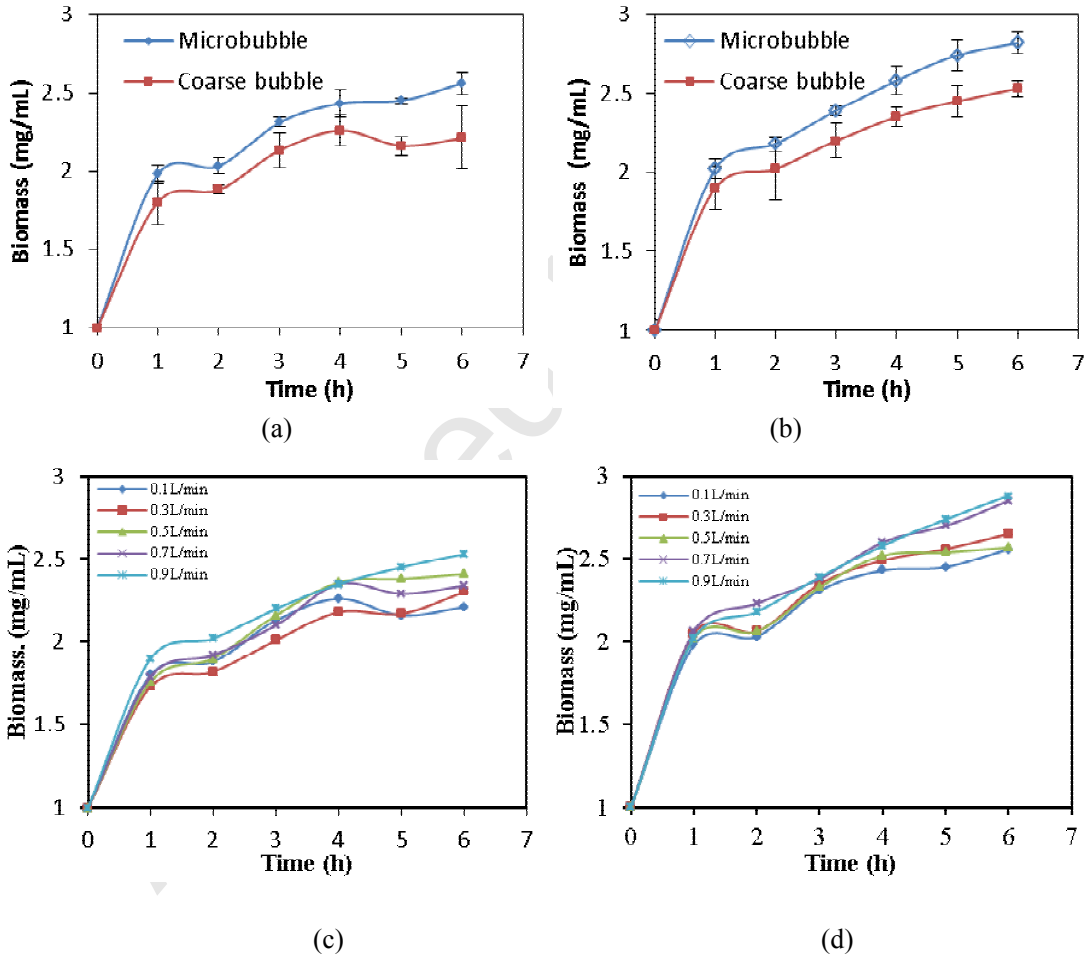


**Figure 4**: Yeast biomass concentration against time. Combined growth plot with microbubble and coarse bubble aeration system at: (a) Lowest flowrate studied – 0.1 L/min. (b) Highest flowrate studied– 0.9 L/min. Result for culture aeration at varying flowrates: (c) With coarse bubbles. (d) With microbubbles. The biomass concentration results achieved in three (3) hours propagation with microbubbles matched the results for coarse bubbles at six (6) hour propagation. The error bar represents standard error for the duplicated tests.

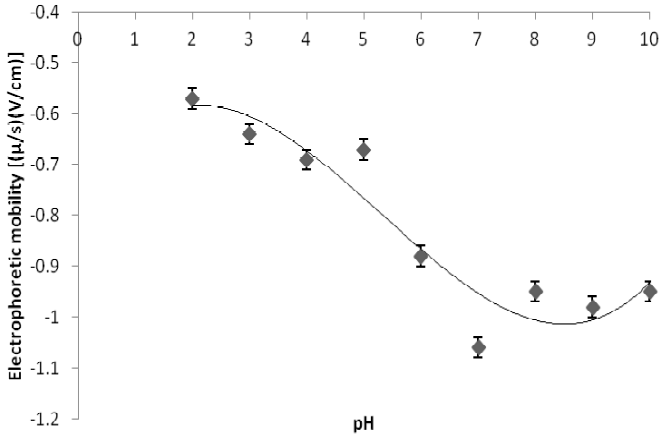


**Figure 5**: Electrophoretic mobility result of yeast cells plotted against varying pHs. Cell surface charge was conducted at $t_0$ hours pre-culture and result show a negative charge across pHs 2-10. Although the IEP was not reached, cells are likely to aggregate and sediment due to the low charge magnitude of the individual cells.

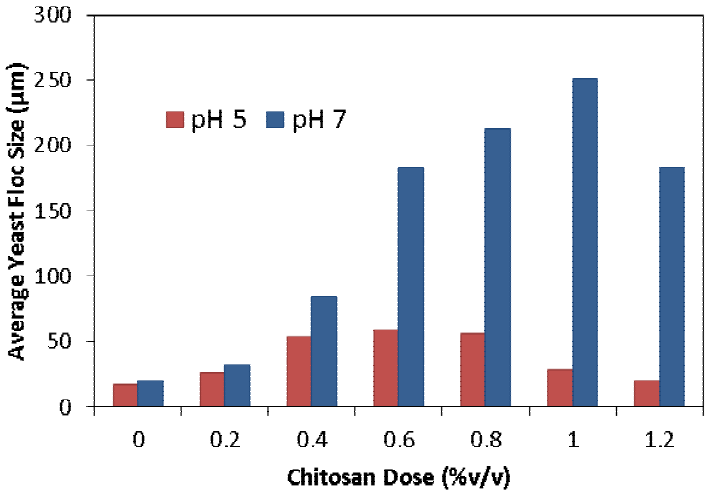


**Figure 6**: Size characterisation of yeast cells before and after treatment with a biological flocculant -- chitosan. Cells aggregated more under higher flocculant dose for both pHs. Also, there was a remarkable difference in the cell floc size at varying pHs, with pH 7 showing a higher threshold to flocculant concentration than pH 5.

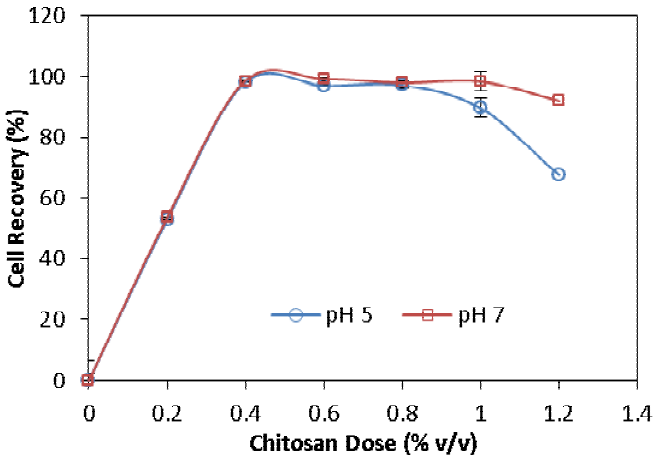


**Figure 7**: Recovery efficiency plot of cells harvested using microbubbles against the biological flocculant - chitosan. Both pH conditions recorded a high percentage yield in recovery with pH 7 exhibiting an increased result. At low chitosan dosage, cells were poorly flocculated leading to low recovery efficiency.